J. Membrane Biol. 198, 125–133 (2004)
DOI: 10.1007/s00232-004-0659-x

The Journal of
Membrane
Biology

Permeant Anions Control Gating of Calcium-dependent Chloride Channels

P. Perez-Cornejo[1,3], **J.A. De Santiago**[2], **J. Arreola**[2,3]
[1]School of Medicine, Universidad Autonoma de San Luis Potosi, 78290 Mexico
[2]Institute of Physics, Universidad Autonoma de San Luis Potosi, 78290 Mexico
[3]Center for Oral Biology, University of Rochester, Medical Center, Rochester, NY 14642, USA

Received: 30 October 2003/Revised: 13 February 2004

Abstract. The effects of external anions (SCN^-, NO_3^-, I^-, Br^-, F^-, glutamate, and aspartate) on gating of Ca^{2+}-dependent Cl^- channels from rat parotid acinar cells were studied using the whole-cell configuration of the patch-clamp technique. Shifts in the reversal potential of the current induced by replacement of external Cl^- with foreign anions, gave the following selectivity sequence based on permeability ratios (P_x/P_{Cl}): $SCN^- > I^- > NO_3^- > Br^- > Cl^- > F^-$ > aspartate > glutamate. Using a continuum electrostatic model we calculated that this lyotropic sequence resulted from the interaction between anions and a polarizable tunnel with an effective dielectric constant of ~23. Our data revealed that anions with $P_x/P_{Cl} > 1$ accelerated activation kinetics in a voltage-independent manner and slowed deactivation kinetics. Moreover, permeant anions enhanced whole-cell conductance (g, an index of the apparent open probability) in a voltage-dependent manner, and shifted leftward the membrane potential-g curves. All of these effects were produced by the anions with an effectiveness that followed the selectivity sequence. To explain the effects of permeant anions on activation kinetics and g_{Cl} we propose that there are 2 different anion-binding sites in the channel. One site is located outside the electrical field and controls channel activation kinetics, while a second site is located within the pore and controls whole-cell conductance. Thus, interactions of permeant anions with these two sites hinder the closing mechanism and stabilize the channel in the open state.

Key words: Ca^{2+}-dependent Cl^- channels — Gating — Anion selectivity — Acinar cells — Permeation

Introduction

It is thought that a rapid Cl^- loss to the luminal side of salivary gland acinar cells is the critical event in the signaling cascade triggered by muscarinic stimulation leading to fluid secretion (Turner, 1993; Cook et al., 1994). In rat parotid glands, Ca^{2+}-dependent Cl^- channels appear to be the exit pathway for Cl^- ions driving fluid secretion (Arreola, Melvin & Begenisich, 1996a; Begenisich & Melvin, 1998; Kidd & Thorn, 2000). Localization of these channels to the apical membrane in acinar cells (Tan, Marty & Trautmann, 1992) suggests that they are exposed to large changes in both extracellular and intracellular [Cl^-] during the active phase of secretion and thus are subject to regulation by the permeant anion itself.

Recent evidence suggests that foreign permeant anions and changes in [Cl^-] affect Ca^{2+}-dependent Cl^- channels present in several cells. In these channels a prominent effect observed by replacing Cl^- with anions like SCN^-, I^-, NO_3^-, or Br^-, is a speeding of the activation kinetics (Evans & Marty, 1986; Ishikawa & Cook, 1993). This effect can also be observed by increasing the internal Cl^- concentration (Pappone & Lee, 1995). On the other hand, Greenwood and Large (1999) reported that in smooth muscle cells, foreign anions slow the decay of Ca^{2+}-dependent Cl^- currents in a voltage-independent manner. The authors suggested that this alteration was brought about by binding of the anions to a site accessible from the external surface of the membrane.

In addition, effects of permeant anions on gating have also been documented in ClC-0, ClC-1 and ClC-2, all voltage-gated Cl^- channels belonging to the ClC Cl^- channel family (Dinudom, Young & Cook, 1993; Chen & Miller, 1996; Pusch et al., 1995, 1999; Fahlke, Dürr & George, 1997; Rychkov et al., 1998). Anion occupancy of the pore has been linked to fast gating in ClC chloride channels (Chen & Miller, 1996; Pusch

Correspondence to: J. Arreola; email: arreola@dec1.ifisica.uaslp.mx

et al., 1995). This observation is supported by crystallographic data (Dutzler, Campbell & MacKinnon, 2003), and by site-directed mutagenesis of a glutamic acid located in the conduction pathway of ClC-0 channels (Dutzler et al., 2003; Traverso, Elia & Pusch, 2003). In this paper, we present evidence showing that permeant anions regulate gating behavior of Ca^{2+}-dependent Cl^- channels in rat parotid acinar cells. Our data show that channel activation was accelerated whilst deactivation was slowed by anions with permeability ratios larger than 1. Additionally, the membrane potential (E_m) needed to reach half-maximum activation of channels was shifted towards more negative values following the selectivity sequence. Thus, our data suggest that the anion permeation mechanism is coupled to the gating machinery of the Ca^{2+}-dependent Cl^- channel.

Materials and Methods

Single-Cell Dissociation

Single acinar cells were dissociated from rat parotid glands as previously described (Arreola, Melvin & Begenesich, 1995). Briefly, glands were dissected from exsanguinated Wistar strain male rats (Charles River, Kingston facility, NY) after CO_2 anesthesia. Glands were minced in Ca^{2+}-free, minimum essential medium (MEM) (Gibco BRL, Gaithersburg, MD) + 1% bovine serum albumin (BSA) (Fraction V, Sigma St. Louis, MO). The tissue was treated for 20 min (37°C) with a 0.02% trypsin solution (MEM Ca^{2+}-free + 1 mM EDTA (ethylenediaminetetraacetic acid) + 2 mM glutamine + 1% BSA). Digestion was stopped with 2 mg/ml of soybean trypsin inhibitor (Sigma) and the tissue was further dispersed by two sequential treatments of 60 min each with collagenase (100 units/ml of type CLSPA, Worthington Biochemical, Freehold, NJ) in MEM Ca^{2+}-free + 2 mM glutamine + 1% BSA. Dispersed cells were centrifuged and washed with basal medium Eagle (BME) (Gibco)/BSA-free. The final pellet was resuspended in BME/BSA-free + 2 mM glutamine and cells were plated onto poly-L-lysine-coated glass coverslips for electrophysiological recordings.

Solutions

The Ca^{2+}-buffered (250 nM free [Ca^{2+}]) pipette solution (Tsien & Pozzan, 1989; Arreola et al., 1996a) contained (in mM): $CaCl_2$ 23.5, Ca-gluconate 2.705, EGTA-TEA 36.205, TEA-F 5, TES 50, pH = 7.3. High concentrations of EGTA (ethyleneglycol-bis-(β-aminoethylether)-N,N,N′N′-tetraacetic acid) and TES (N-tris(hydroxymethyl)methyl-2-aminoethanesulphonic acid) buffers assured control of both Ca^{2+} and H^+ concentrations during the course of these experiments. Monovalent cations were substituted with TEA^+ (tetraethylammonium) in both the internal and external solutions to avoid cationic currents. The [Cl^-] in the internal (pipette) solution was 47 mM, 40 mosm kg^{-1} more hypotonic than the external solutions, to avoid opening of swelling-activated Cl^- channels (Arreola et al., 1995; Arreola, Melvin & Begenesich, 1996b). The external solutions (326 mosm kg^{-1}) had the following composition (in mM): TEA-X 135 (X = SCN^-, I^-, NO_3^-, Br^-, Cl^- F^-, aspartate, glutamate), $CaCl_2$ 0.5, TES 20, D-mannitol 45, pH = 7.3. Currents were recorded after a period of 4 min or longer subsequent to achieving the whole-cell configuration.

Whole-Cell Recording

The whole-cell configuration of the patch-clamp technique (Hamill et al., 1981) was used to record Cl^- currents from single parotid acinar cells. Glass pipettes had 1–2 MΩ resistance when filled with the internal solution. The bath chamber was grounded using an Ag-AgCl pellet and a 1 M CsCl agar bridge. Liquid junction potentials of +6 mV were experimentally determined (Neher, 1992) and E_m was corrected for this value. Pipette and cell membrane capacitative transients were subtracted from the records by the amplifier circuitry before sampling. Whole-cell Cl^- currents were recorded using a PC-501A patch-clamp amplifier (Warner Instrument, Hamden, CT). Digital-to-analog and analog-to-digital converters (12 bits) were used to generate the stimulus protocols and to sample the currents. E_m was changed from −106 to +94 mV in 20 mV steps by delivering 2.5 s long square pulses every 10 s from a holding potential of −56 mV. Except where indicated, currents were filtered at 500 Hz using an 8-db/decade low-pass Bessel filter and sampled at 100 Hz using custom design software.

Chemicals

EGTA, $CaCl_2$ and TEA-Cl were purchased from Fluka (Buchs, Switzerland). TES, D-mannitol, TEA-F, Ca-$(gluconate)_2$ and other inorganic salts were obtained from either Sigma or Fluka. The EGTA-TEA stock was prepared by mixing equimolar concentrations of EGTA with TEAOH and then pH was adjusted to 7.0.

Analysis

Steady-state current-voltage relations were constructed using the absolute amplitude of the currents measured at the end of the 2.5 s test pulse. The resulting relationships were fitted to a 4th order polynomial and the reversal potentials were obtained by extrapolation. Mean ± SEM values are plotted or given.

The permeability ratios (P_x/P_{Cl}) were calculated using the Goldman-Hodgkin-Katz equation:

$$\frac{P_x}{P_{Cl}} = e^{zF\Delta Er/RT} \tag{1}$$

where z is the ion valence, F is the Faraday constant, R is the gas constant, T is the temperature and ΔE_r is the shift of reversal potential caused by replacing external Cl^- with anion X. Whole-cell Cl^- conductance (g) was calculated as:

$$g = \frac{I_{Cl}}{E_m - E_r} \tag{2}$$

where E_m is the membrane voltage and E_r is the current reversal potential. The resulting conductances were normalized to the conductance observed at +94 mV as described previously (Arreola et al., 1996a), plotted as a function of membrane voltage and fit to a Boltzmann distribution function:

$$g = \frac{G_{max} - G_{min}}{1 + e^{(E_m - E_{0.5})/s}} + G_{min} \tag{3}$$

where G_{max} (equal to 1) and G_{min} are the maximum and minimum normalized conductances, respectively, $E_{0.5}$ is the membrane voltage necessary to obtain 50% of G_{max}, and the parameter s controls the voltage sensitivity of the conductance. This curve will be refered to as the activation curve. The normalized g represents an index of the apparent open probability of the channel, which includes the single-channel conductance and the fraction of open channels. The relationship $\Delta E_{0.5}$ and P_x/P_{Cl} was fit to a Hill equation:

$$\Delta E_{0.5} = \Delta E_{0.5\max}/1 + [K/P_x/P_{Cl}]^n \quad (4)$$

where $\Delta E_{0.5\max}$ is the maximum value of $\Delta E_{0.5}$, K is a constant and n is a parameter that controls the steepness of the curve.

Results

Selectivity of Ca^{2+}-dependent Cl^- Channels

Anion selectivity was determined from whole-cell experiments as shown in Fig. 1. Panel *A* shows whole-cell Cl^- currents recorded from −106 to +94 mV in 20 mV increments from a holding potential of −56 mV. In these experiments, using 250 nM free $[Ca^{2+}]_i$, we recorded an instantaneous current at the onset of the voltage pulse, suggesting that a fraction of Cl^- channels was already open at the holding potential. Hyperpolarizing steps elicited small steady-state currents, whereas depolarizing steps elicited large currents with a slow activation time course. Upon repolarization to −56 mV, a large tail current that followed a monoexponential time course was recorded. In Fig. 1*C* the characteristic outward rectification of the current-voltage relationship for control records is shown. Overall current-voltage relationships recorded were identical to those previously described by Arreola et al. (1996a), in rat parotid acinar cells. Panel *B* shows whole-cell currents recorded from the same cell shown in panel *A* after complete substitution of the external Cl^- with SCN^-. Under these conditions the traces display several distinctive characteristics: a) larger currents; b) a faster activation time course; and c) slower tail currents. The corresponding current-voltage relationship in the presence of SCN^- is shown in panel *D*. Although the outward rectification is preserved, a large shift on the reversal potential is clearly seen. This indicated a larger permeability of SCN^- compared to Cl^-. A similar pattern was observed when the external Cl^- was replaced with $NO3^-$, I^-, and Br^-, but not with F^-.

A selectivity sequence for Ca^{2+}-dependent Cl^- channels was calculated using the Goldman, Hodgkin and Katz equation (Eq. 1) and values from reversal potential shifts. The sequence was SCN^- (4.3 ± 0.4; $n=4$) > I^- (2.6 ± 0.1; $n=4$) > NO_3^- (2.0 ± 0.07; $n=4$) > Br^- (1.6 ± 0.08; $n=4$) > Cl^- (1) > F^- (0.3 ± 0.04; $n=3$) > aspartate (0.1 ± 0.02; $n=4$) > glutamate (0.05 ± 0.02; $n=3$). This selectivity sequence is similar to that determined for Ca^{2+}-dependent Cl^- channels from other preparations, including rat lachrymal, skeletal muscle, rat epididymal cells, insulin secreting cells, sheep parotid acinar cells, mouse duct cells, and *Xenopus* oocytes (Evans & Marty, 1986; Hume & Thomas, 1989; Huang et al., 1993; Kozak & Logothetis, 1997; Ishikawa & Cook, 1993; Qu & Hartzell, 2000). Recently, it has been shown that the lyotropic anion selectivity of the cystic fibrosis transmembrane conductance regulator (CFTR) chloride channel can be reproduced using a continuum electrostatic model that assumes an interaction between a polarizable pore with an effective dielectric constant of 19 and the permeant anions (Smith et al., 1999). On the other hand, anion permeation through Ca^{2+}-dependent Cl^- channels in *Xenopus* oocytes cannot be entirely reproduced by this model, suggesting that the mechanism of anion permeation in these channels differs from the mechanism used by CFTR channels (Qu & Hartzell, 2000). Nonetheless, here we use the same continuum electrostatic model to analyze anion permeation in Ca^{2+}-dependent Cl^- channels from rat parotid acinar cells (Smith et al., 1999). Barrier heights ($\Delta(\Delta G)_{barrier}$) for different anions relative to SCN^- were calculated as

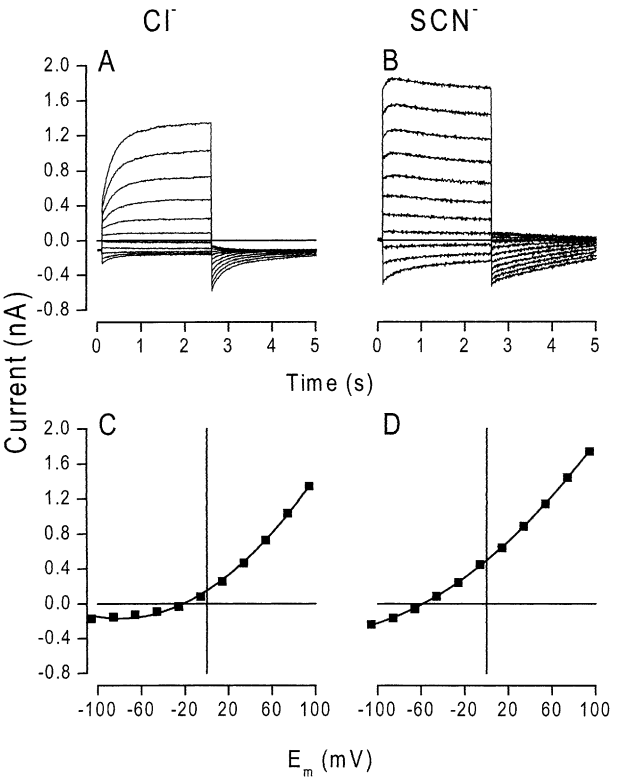

Fig. 1. Activation of Ca^{2+}-dependent Cl^- channels in the presence of external Cl^- and SCN^-. Whole-cell currents recorded before (*A*) and after (*B*) 100% replacement of external Cl^- with SCN^-. (*C* and *D*) Corresponding current-voltage relationships obtained by plotting current magnitude at the end of the pulses against membrane voltage. Continuous lines are polynomial fits used to determine the reversal potentials by interpolation.

$$\frac{P_x}{P_{SCN}} = e^{(-\Delta(\Delta G)_{barrier}/RT)} \quad (5)$$

and the Born energy of hydration (ΔG_{hyd}) was calculated as:

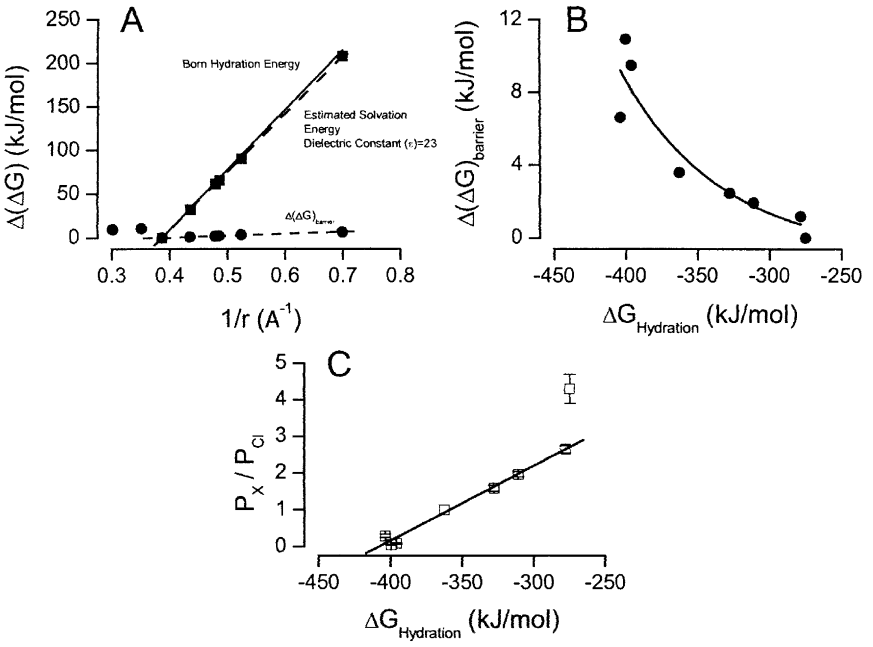

Fig. 2. Analysis of anion selectivity by Ca^{2+}-dependent Cl^- channels. (*A*) ΔG_{hyd} (*continuous line*), $\Delta G_{solvation}$ (*squares*), $\Delta(\Delta G_{barrier})$ (*circles*) as a function of inverse radius. Dashed line through $\Delta G_{solvation}$ data was used to calculate the slope from which a dielectric constant of ~23 was estimated. *See* text for details of calculations. (*B*) Exponential relationship between ΔG_{hyd} and $\Delta(\Delta G_{barrier})$. (*C*) Linear relationship between P_x/P_{Cl} and ΔG_{hyd}. *See* text for details of analysis.

$$\Delta G_{hyd} = -\frac{K}{2r}\left(1 - \frac{1}{\varepsilon}\right) \quad (6)$$

where $K = 1389$ ÅkJ/mol, r is the ion radius and ε is the dielectric constant of water. Figure 2*A* shows the relationship between $\Delta(\Delta G)_{barrier}$, ΔG_{hyd} or solvation energy (obtained as $\Delta G_{hyd} - \Delta(\Delta G)_{barrier}$) and $1/r$. As the anion size increased, $\Delta(\Delta G)_{barrier}$ linearly decreased, resulting in an increased permeability. From the slope of solvation energy vs $1/r$, an effective dielectric constant of ~23 was calculated. As a first approximation, this analysis provides an explanation for the selectivity of Ca^{2+}-dependent Cl^- channels from rat parotid acinar cells. However the relationship between $\Delta(\Delta G)_{barrier}$ and ΔG_{hyd} (Marcus, 1997) is exponential (Fig. 2*B*), similar to that observed in the *Xenopus* oocyte (Qu & Hartzell, 2000), arguing that the selectivity of Ca^{2+}-dependent Cl^- channels can not be fully accounted for by this model. Figure 2*C* shows that, with the exception of P_{SCN}/P_{Cl}, the permeability ratios of the tested anions were nearly linearly related to ΔG_{hyd}.

Effects of Permeant Anions on Channel Gating

Figure 1 shows that time courses of activation and deactivation of whole-cell currents are strongly affected by SCN^-. In order to determine a time constant of activation ($\tau_{activation}$), that quantitatively describes the effects of different permeant anions on activation kinetics, whole-cell Cl^- currents were fit with a single exponential function. This analysis was restricted to permeant anions that at positive potentials gave large enough currents to have reliable fits. With external F^-, only one cell showed sufficiently large outward currents to do the fitting procedure, whereas with aspartate and glutamate, small currents were recorded from all cells tested, which precluded the estimation of $\tau_{activation}$ for these three anions. Figure 3 shows the effects of different anions on channel kinetics. Panels *A* and *B* depict normalized currents in the presence of Cl^- (control, *thin traces*) and after replacing Cl^- with SCN^- and NO_3^- (*thick traces*), respectively. Control traces in the presence of Cl^- displayed slower onset kinetics than those in the presence of the tested anion. In addition to effects on activation, SCN^- and NO_3^- also slowed deactivation of currents. The effects of SCN^- were always larger than those observed with NO_3^-. On panel *C*, the $\tau_{activation}$ of whole-cell currents in the presence of the tested anions relative to control currents is shown as a function of E_m. Two observations are evident from this graph: a) the accelerating effects of permeant anions are independent of E_m, and *b*) the relative accelerating effect induced by the tested anions followed the sequence $SCN^- > I^- \geq NO_3^- > Br^- > F^-$, which is identical to the selectivity sequence determined from reversal potentials (*see* above).

The effects of the permeant anions on closing kinetics were studied by recording the tail currents at a repolarizing potential of −56 mV and then fitting a double-exponential function to the raw current traces. From this fit we determined that permeant anions only affected the slow time constant. This time constant relative to control is plotted in Fig. 3 panel *D*. The ability of permeant anions to slow down deactivation kinetics followed the sequence $SCN^- > I^- \geq NO_3^- > Br^- > F^-$. This sequence is identical to that

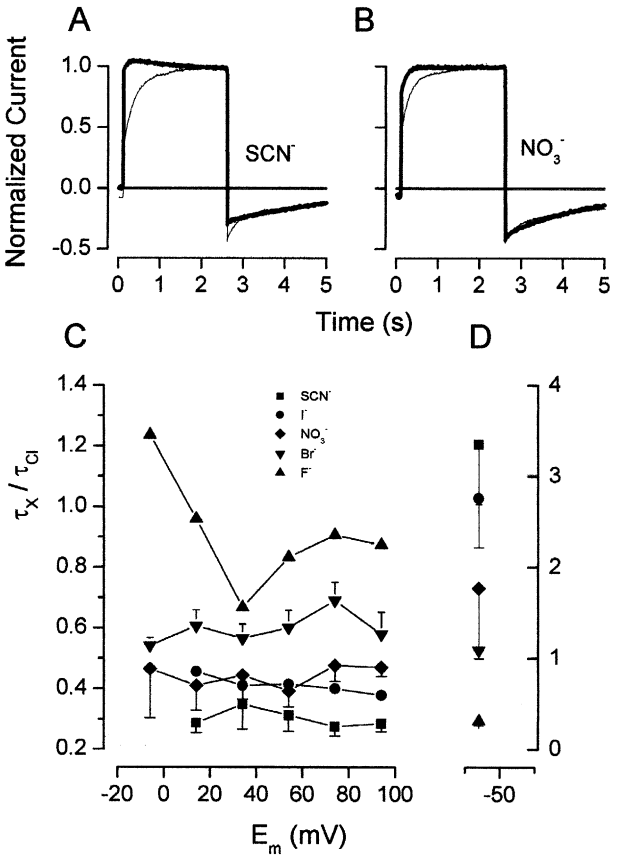

Fig. 3. Activation and deactivation kinetics of Ca^{2+}-dependent Cl^- channels. Panels *A* and *B* show normalized single traces recorded at +94 mV in the presence of external Cl^- (*thin traces*) and in the presence of SCN^- and NO_3^- (*thick traces*), respectively. (*C*) Activation time constants in the presence of different external anions normalized to that in the presence of Cl^- as a function of E_m. (*D*) Deactivation time constant at −56 mV determined in the presence of different external anions and normalized to that determined in the presence of Cl^-.

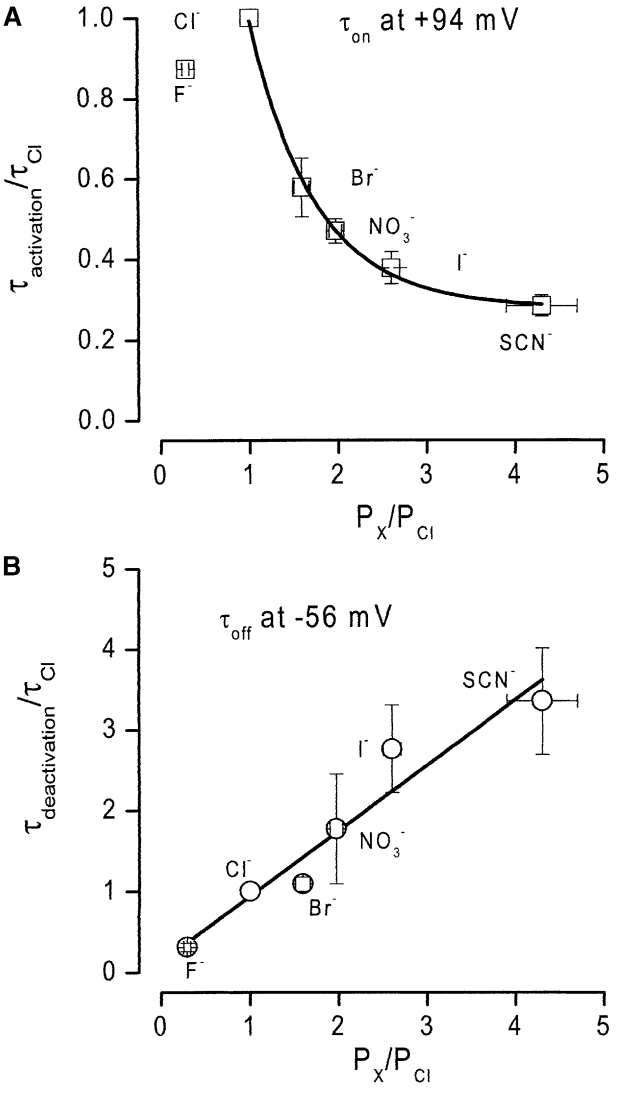

Fig. 4. Relationship between activation and deactivation kinetics and permeability ratios. Activation (*A*) and deactivation (*B*) time constants determined at +94 and −56 mV, respectively, calculated in the presence of different anions were normalized to values calculated in the presence of Cl^-. Continuous lines are exponential (*A*) and linear (*B*) fits.

determined from reversal potential shifts and activation kinetics (*see* Fig. 3*C*).

Our results thus far indicate that selectivity and gating are intimately linked. Additional evidence to support this view is shown in Fig. 4. This figure depicts the relationship between activation (*A*) or deactivation (*B*) time constants and permeability ratios for SCN^-, I^-, NO_3^-, Br^- and F^-. Data were normalized to the time constants obtained in the presence of external Cl^-. The results show that activation kinetics at +94 mV (*A*) were accelerated about 4-fold by SCN^- and about 2-fold by NO_3^-. These numbers are nearly identical to the permeability ratios of these anions. Moreover, acceleration of the activation followed a nearly exponential relationship (*continuous line*) with the permeability ratio. In contrast, the deactivation time constant at −56 mV was slowed 3-fold by SCN^- and about 2 fold by NO_3^- (Fig. 4*B*) and it was linearly related to permeability ratios.

The voltage-dependence of apparent open probability, assessed as the membrane voltage needed to reach activation of 50% of the total number of channels ($E_{0.5}$), was facilitated by permeant anions. $E_{0.5}$ under different ionic compositions was determined from fitting the normalized whole-cell conductance with a Boltzmann equation (Eq. 3). Normalized conductance was obtained by transforming whole-cell currents to conductance using Eq. 2. Figure 5*A* shows the effects of permeant anions on the voltage-dependence of whole-cell conductance. Replacing external Cl^- with I^- or Br^- shifted the E_m-conductance relationship towards more negative voltages by −34.4 and −22.5 mV, respectively. The

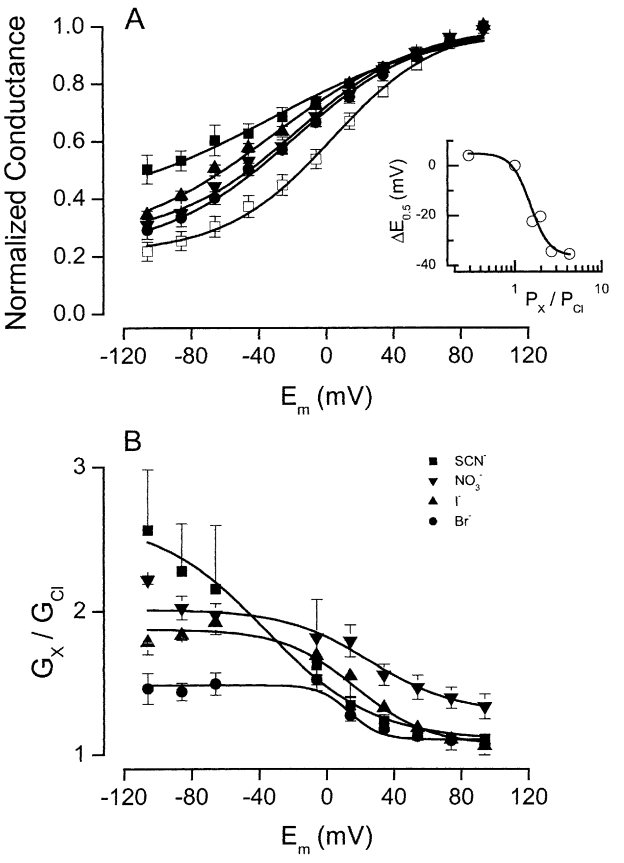

Fig. 5. Effects of foreign anions on conductance. (*A*) Normalized conductance as a function of E_m determined in the presence of external Cl^- (*empty squares*) and in the presence of SCN^- (*filled squares*), NO_3^- (*down triangles*), I^- (*up triangles*), and Br^- (*filled circles*). Whole-cell conductance values were normalized to that obtained at +94 mV. Continuous lines are the fits with the Boltzmann equation to determine E_m needed to reach 50% of maximum conductance ($E_{0.5}$). $E_{0.5}$ values were used to determine shifts induced by anionic substitutions. *Inset*: $E_{0.5}$ shifts (*empty circles*) as a function of permeability ratios. Data was fitted with Eq. 4, using parameters $K = 1.5$ and $n = 4$. (*B*) G_x/G_{Cl} ratios as a function of E_m. Whole-cell conductance values obtained at each E_m for the test anion were divided by their corresponding conductance obtained in the presence of external Cl^-.

inset in Fig. 5*A* shows the relationship between the shifts in $E_{0.5}(\Delta E_{0.5})$ induced by permeant anions and their corresponding permeability ratios. The data followed a sigmoid relationship that was fitted using Eq. 4 with $K=1.4$ and had a coefficient $n=4$. The order of potency of the anions to affect $E_{0.5}$ followed the same pattern as that described for activation and deactivation kinetics.

It has been shown that permeant anions facilitate activation of ClC-0 and volume-sensitive Cl^- channels by interacting with the channel in a voltage-dependent manner, probably interacting with the conduction pathway itself (Pusch et al., 1995; Voets, Droogmans & Nilius, 1997). Figure 5*B* shows that permeant anions increased in a voltage-dependent manner the whole-cell conductance of Ca^{2+}-dependent Cl^- channels. Whole-cell conductance in the presence of the test anion was calculated using equation 2, and then divided by the whole-cell conductance obtained in the presence of Cl^-. The resulting ratios were plotted as a function of E_m in Fig. 5*B*. As E_m became more negative, the ratio of conductances approached a maximum that depended on the external anion tested and followed the same order as the selectivity sequence determined from reversal potentials. At +24 mV, the ratio G_{SCN}/G_{Cl} sharply decreased below G_{NO3}/G_{Cl} and G_I/G_{Cl}, and this resulted in an inversion of the selectivity sequence ($NO_3^- > I^- > SCN^- > Cl^-$). At positive E_m, the ratio of conductances nearly reached 1 for all the anions, but did not decrease below 1.

Figure 5 suggests that the effects of permeant anions on activation are likely to involve interactions within the pore itself. Mixtures of SCN^-/Cl^- or Br^-/Cl^- were used to determine the presence of any anomalous mole fraction behavior of E_r, $\Delta E_{0.5}$, slope conductance and time constants of activation, a behavior directly associated with interactions between the ions and the pore. However, none of these parameters displayed an obvious anomalous mole fraction effect (*data not shown*). E_r shifted with a constant permeability ratio, as predicted by the Goldman-Hodgkin-Katz equation; $\Delta E_{0.5}$ shifted leftward, as described above; the slope conductance increased in a sigmoid fashion without signs of blockade, and the time constants were accelerated as shown above.

Discussion

The data presented in this paper show that the presence of external, permeant anions have profound effects on the kinetics and voltage-dependent activation of Ca^{2+}-dependent Cl^- channels from rat parotid acinar cells. Specifically, anions that have a permeability ratio larger than 1 accelerated transitions leading to the open state, slowed the closing rate and facilitated the voltage dependency of apparent open probability of the channel. These effects could prolong the time residence of the channel in the open state. All these effects on gating are related to permeability ratios, suggesting a direct cause-effect relationship between the two processes. Mechanisms such as these could potentially be operating during acinar-cell fluid secretion, since about 50% of the cell chloride content (and a fraction of HCO_3^-) is rapidly lost after the muscarinic stimulation that produces fluid secretion (Foskett & Melvin, 1984; Foskett, 1990). Thus, Cl^- and HCO_3^- ions would transiently accumulate outside the apical membrane and potentially control channel gating.

Ca^{2+}-dependent Cl^- channels from rat parotid acinar cells show the same lyotropic selectivity sequence ($SCN^- > I^- > NO_3^- > Br^- > Cl^- > F^-$ > aspartate > glutamate) as that determined for volume-sensitive Cl^- channels (Arreola et al., 1995), CFTR (Tabcharani, Linsdell & Hanrahan, 1997), outwardly rectifying Cl^- channels in T84 cells (Halm & Frizzell, 1992) and GABA and glycine activated Cl^- channels (Bormann, Hamill & Sakmann, 1987). In all these Cl^- channels, permeability ratios are linearly related to the hydration energy of the anions, which suggests a common mechanism for anion selection based on a pore that has weak field strength binding sites (Dawson et al., 1999). Consequently, in all these Cl^- channels the hydration energy plays a dominant role in permeation. Permeation data was analyzed according to a polarizable pore model for CFTR (Smith et al., 1999). A similar analysis applied here for the Ca^{2+}-dependent Cl^- channel hint at a pore with an effective dielectric constant of ~23. This value approximates to 19 and 20.7, which are values determined for CFTR and Ca^{2+}-dependent Cl^- channels from *Xenopus* oocytes, respectively (Smith et al., 1999; Qu & Hartzell, 2000). Still, this analysis does not take into consideration polyatomic anions with permeability ratios lower than those observed for F^-. Although the relationship between ΔG_{hyd} and P_x/P_{Cl} appears to be linear, the relationship between $\Delta(\Delta G)_{barrier}$ and ΔG_{hyd} is not. Despite these limitations, the observed anion selectivity in Ca^{2+}-dependent Cl^- channels appears to display some of the important characteristics expected of anion passage through a polarizable pore that mimics anion solvation.

Ca^{2+}-dependent Cl^- channels from *Xenopus* oocytes are affected by lyotropic anions when these are applied on the intracellular side of the plasma membrane. The substitution of 150 mM intracellular Cl^- with SCN^- resulted in significant acceleration of activation and a decrease in the K_d for Ca^{2+} at 0 mV that went from 279 to 131 nM (Qu & Hartzell, 2000). However, little or no effect was seen on channel deactivation, contrary to the results reported here. Although we cannot rule out intracellular effects of foreign anions on channel gating due to accumulation during depolarizations, the following reasons argue that this contribution is likely to be minor in our experiments. First, accumulation of permeant anions during depolarization would not be sufficient to reach the concentration needed (150 mM) to decrease the K_d for Ca^{2+} at 0 mV (as mentioned above). Second, changes were made in the ionic composition of the external medium whilst the intracellular Ca^{2+} and H^+ were strongly buffered. Third, the effects of external anions were observed at negative voltages (*data not shown*) where Cl^- ions are moving outwardly and little intracellular accumulation of external anions is expected. Fourth, all the effects readily reverted upon washing, contrary to the effects observed in lachrimal glands after prolonged exposure to I^- (Evans & Marty, 1986). Moreover, no effects on Ca^{2+}-dependent Cl^- channel deactivation were reported in cells dialyzed with I^- (Greenwood & Large, 1999). Thus, the majority of the effects on activation kinetics reported here can be readily explained by direct interaction of permeant anions with the channel protein. This interaction likely takes place with an external portion of the protein and does not interfere with Ca^{2+} affinity, as has been shown in smooth muscle (Greenwood & Large, 1999). This conclusion is supported by the voltage-independent acceleration of activation time constants (Fig. 3*C*), which is interpreted as the result of anions interacting with the channel outside the electrical field, presumably with a binding site located on the extracellular side of the pore.

Permeant anions also slowed deactivation, with a net result similar to the "foot in the door" effect described for potassium channels (Armstrong, 1971). In the context of this hypothesis, anions with easy access to the selectivity filter/permeation pathway of the pore have rapid access to the gate, which allows them to keep the gate in the open state for prolonged periods of time. Although it is unclear whether the anion binding site regulating channel activation kinetics is also regulating deactivation kinetics, our data demonstrate that both gating mechanisms are controlled by the permeant anions with a potency that follows the permeability sequence.

The effects of permeant anions on gating are not unique to Ca^{2+}-dependent Cl^- channels. In fact, these effects have been extensively studied in voltage-activated Cl^- channels belonging to the ClC family (Pusch et al., 1995, 1999; Chen & Miller, 1996; Rychkov et al., 1996). For instance, the open probability of ClC-0 channels is increased when the external Cl^- concentration is increased. This effect results from the direct interaction of Cl^- ions with an external site in the channel protein during the closed state. In turn, this interaction accelerates the transition rate leading to the open state (Chen & Miller, 1996). Pusch et al., (1995) demonstrated that in ClC-0, both $E_{0.5}$ and normalized conductance exhibit anomalous mole fraction effects. This evidence suggests that the gating process is tightly coupled to the permeation of Cl^- ions. Although our data does not show an anomalous mole fraction effect (strictly a pore property) with SCN^- or Br^-, this does not rule out the participation of events taking place in the pore of Ca^{2+}-dependent Cl^- channels during the permeation process. Interactions between ions and the channel pore appeared clear when the effects of the anions on the voltage-dependency of whole-cell conductance were examined. Here, permeant anions shifted the voltage dependency of activation and increased the relative whole-cell conductance in a voltage-dependent man-

ner. This supports the idea that permeant anions interact by binding to the channel within the electrical field, which resulted in a voltage-dependent facilitation of whole-cell conductance at negative voltages. Further experiments are necessary to determine alterations on single-channel conductance and open probability caused by these anions.

In summary, the intimate relationship between permeability ratios and activation/deactivation kinetics as well as apparent open probability (estimated by $E_{0.5}$) suggests coupling of permeation and gating mechanisms. The complex effects of permeant anions on Ca^{2+}-dependent Cl^- channels suggest the presence of at least two binding sites for anions. Thus, we propose that one site is located outside the pore and controls activation kinetics, while a second site is located within the electrical field and controls the voltage-dependence of the apparent open probability.

We thank Dr. David Giovanucci for critical reading this manuscript. This work was supported in part by grants 5-25881N and ER026 (CONACyT, Mexico), and DE-09692 (NIH, USA).

References

Armstrong, C. 1971. Interaction of tetraethylammonium ion derivatives with the potassium channels of giant axons. *J. Gen. Physiol.* **58:**413–437

Arreola, J., Melvin, J.E., Begenisich, T. 1995. Volume-activated chloride channels in rat parotid acinar cells. *J. Physiol.* **484:**677–687

Arreola, J., Melvin, J.E., Begenisich, T. 1996a. Activation of calcium-dependent chloride channels in rat parotid acinar cells. *J. Gen. Physiol.* **108:**35–47

Arreola, J., Melvin, J.E., Begenisich, T. 1996b. Three distinct chloride channels control anion movement in rat parotid acinar cells. *J. Physiol.* **490:**351–362

Begenisich, T., Melvin, J.E. 1998. Regulation of chloride channels in secretory epithelia. *J. Membrane Biol.* **163:**77–85

Bormann, J., Hamill, O.P., Sakmann, B. 1987. Mechanism of anion permeation through channels gated by glycine and γ-aminobutyric acid in mouse cultured spinal neurones. *J. Physiol.* **385:**243–286

Chen, T.Y., Miller, C. 1996. Nonequilibrium gating and voltage dependence of the ClC-0 Cl^- channel. *J. Gen. Physiol.* **108:**237–250

Cook, D.I., Van Lennep, E.W., Roberts, M.L., Young, J.A. 1994. Secretion by the major salivary glands. *In:* Johnson, L.R. (editor) *Physiology of the Gastrointestinal Tract*. Raven Press, NY, pp 1061–1117

Dinudom, A., Young, J.A., Cook, D.I. 1993. Na^+ and Cl^- conductances are controlled by cytosolic Cl^- concentration in the intralobular duct cells of mouse mandibular glands. *J. Membrane Biol.* **135:**289–295

Dawson, D.C., Smith, S.S., Mansoura, M.K. 1999. CFTR: Mechanism of anion conduction. *Physiol Rev.* **79:**S47–S75

Dutzler, R., Campbell, E.B., MacKinnon, R. 2003. Gating the selectivity filter in ClC chloride channels. *Nature* **300:**108–112

Evans, M.G., Marty, A. 1986. Calcium-activated chloride currents in isolated cells from rat lachrymal gland. *J. Physiol.* **378:**437–460

Fahlke, C., Dürr, C., George, Jr., A.L. 1997. Mechanism of ion permeation in skeletal muscle chloride channels. *J. Gen. Physiol.* **110:**551–564

Foskett, J.K. 1990. $[Ca^{2+}]_i$ modulation of Cl^- content controls cell volume in single salivary acinar cells during fluid secretion. *Am. J. Physiol.* **259:**C998–C1004

Foskett, J.K., Melvin, J.E. 1984. Activation of salivary secretion: coupling of cell volume and $[Ca^{2+}]_i$ in single cells. *Science* **244:**1582–1585

Greenwood, I.A., Large, W.A. 1999. Modulation of decay of Ca^{2+}-activated Cl^- currents in rabbit portal vein smooth muscle cells by external anions. *J. Physiol.* **516:**365–376

Halm, D.R., Frizzell, R.A. 1992. Anion permeation in an apical membrane chloride channel of a secretory epithelial cell. *J. Gen. Physiol* **99:**339–366

Hamill, O.P., Marty, A., Neher, E., Sakmann, B., Sigworth, F.J. 1981. Improved patch-clamp techniques for high-resolution current recording from cells and cell-free membrane patches. *Pfluegers Arch-Eur. J. Physiol.* **391:**85–100

Huang, S.J., Fu, W.O., Chung, Y.W., Zhou, T.S., Wong, P.Y.D. 1993. Properties of cAMP-dependent and Ca^{2+}-dependent whole-cell Cl^- conductances in rat epididymal cells. *Am. J. Physiol.* **264:**C794–C802

Hume, R.I., Thomas, S.A. 1989. A calcium- and voltage-dependent chloride current in developing chick skeletal muscle. *J. Physiol.* **417:**241–261

Ishikawa, T., Cook, D.I. 1993. A Ca^{2+}-activated Cl^- current in sheep parotid secretory cells. *J. Membrane Biol.* **135:**261–271

Kidd, J.F., Thorn, P. 2000. Intracellular Ca^{2+} and Cl^- channel activation in secretory cells. *Ann. Rev. Physiol.* **62:**493–513

Kozak, J.A., Logothetis, D.E. 1997. A calcium-dependent chloride current in insulin-secreting bTC-3 cells. *Pfluegers Arch-Eur. J. Physiol.* **433:**679–690

Marcus, Y. 1997. *Ion Properties*. Marcel Dekker, New York.

Neher, E. 1992. Correction for liquid junction potentials in patch clamp experiments. *Methods Enzymol* **207:**123–131

Pappone, P., Lee, S.C. 1995. α-Adrenergic stimulation activates a calcium-sensitive chloride current in brown fat cells. *J. Gen. Physiol.* **106:**231–258

Pusch, M., Ludewig, U., Rehfeldt, A., Jentsch, T.J. 1995. Gating of the voltage-dependent chloride channel ClC-0 by the permeant anion. *Nature* **373:**527–531

Pusch, M., Jordt, S.E., Stein, V., Jentsch, T.J. 1999. Chloride dependence of hyperpolarization-activated chloride channel gates. *J. Physiol.* **515:**341–353

Qu, Z., Hartzell, H. 2000. Anion permeation in Ca^{2+}-activated Cl^- Channels. *J. Gen. Physiol.* **116:**825–844

Rychkov, G.Y., Pusch, M., Astill, D.S., Roberts, M.L., Jentsch, T.J., Bretag, A.H. 1996. Concentration and pH dependence of skeletal muscle chloride channel ClC-1. *J. Physiol.* **497:**423–435

Rychkov, G.Y., Pusch, M., Roberts, M.L., Jentsch, T.J., Bretag, A.H. 1998. Permeation and block of the skeletal muscle chloride channel ClC-1 by foreign anions. *J. Gen. Physiol.* **111:**653–665

Smith, S.S., Steinle, E.D., Meyerhoff, M.E., Dawson, D.C. 1999. Cystic fibrosis transmembrane conductance regulator: physical basis for lyotropic anion selectivity patterns. *J. Gen. Physiol.* **114:**799–817

Tabcharani, J.A., Linsdell, P., Hanrahan, J.W. 1997. Halide permeation in wild-type and mutant cystic fibrosis transmembrane conductance regulator chloride channels. *J. Gen. Physiol.* **110:**341–354

Tan, Y.P., Marty, A., Trautmann, A. 1992. High density of Ca^{2+}-dependent K^+ and Cl^- channels on the luminal

membrane of lacrimal acinar cells. *Proc. Nat. Acad. Sci. USA* **89:**11229–11233

Traverso, S., Elia, L., Pusch, M. 2003. Gating competence of constitutively open ClC-0 mutants revealed by the interaction with a small organic inhibitor. *J. Gen. Physiol.* **122:**295–306

Tsien, R., Pozzan, T. 1989. Measurements of cytosolic free Ca^{2+} with Quin 2. *Methods Enzymol.* **172:**230–262

Turner, R.J. 1993. Ion transport related to fluid secretion in salivary glands. *In:* Dobrosielski-Vergona, K. (editor) Biology of Salivary Glands. CRC Press Inc., Salem, MA, pp 105–127

Voets, T., Droogmans, G., Nilius, B. 1997. Modulation of voltage-dependent properties of a swelling-activated Cl^- current. *J. Gen. Physiol.* **110:**313–325